

Polyacrylate-Assisted Size Control of Silver Nanoparticles and Their Catalytic Activity

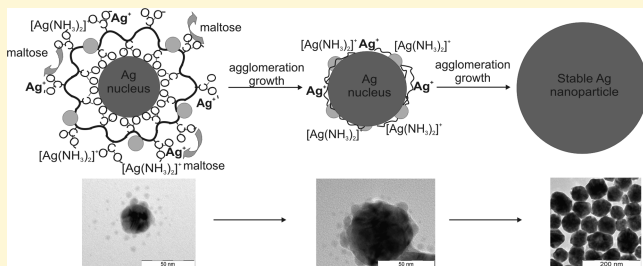
Aleš Panáček,[†] Robert Prucek,[†] Jan Hrbáč,[‡] Tat'jana Nevečná,[‡] Jana Šteffková,[‡] Radek Zbořil,[†] and Libor Kvítek^{*,†}

[†]Regional Centre of Advanced Technologies and Materials, Department of Physical Chemistry, Faculty of Science, Palacky University in Olomouc, 17. listopadu 12, 771 46 Olomouc, Czech Republic

[‡]Department of Physical Chemistry, Faculty of Science, Palacky University in Olomouc, 17. listopadu 12, 771 46 Olomouc, Czech Republic

Supporting Information

ABSTRACT: In this work, a simple one-step method of silver nanoparticle (NPs) preparation with controlled size is introduced. Silver NPs were prepared by reduction of $[\text{Ag}(\text{NH}_3)_2]^+$ complex cation by D-maltose in the presence of low concentrations (1×10^{-10} mol/L to 1×10^{-7} mol/L) of high-molecular-weight poly(acrylic acid) (PAA). This modification of the reduction reaction results in managing of the prepared silver nanoparticles' size in the range from 28 nm (the reaction system without PAA) to 77 nm (system with the highest used PAA concentration). The presence of poly(acrylic acid) influences both nucleation process and also the subsequent stage of nanoparticle growth. The rate of nuclei formation by homogeneous nucleation is affected by PAA due to the formation of the strong complex with silver ions which results in a prolongation of the initiation phase of the reduction process proportionally to PAA concentration. The formation of the adsorption layer of PAA on the surface of the emerging silver nuclei prevents the direct contact between silver ions and nuclei, which is necessary for continuation of the nuclei growth via heterogeneous catalytical mechanism. Because of this restriction, the silver nuclei grow up to their final size by the aggregation mechanism. The as-prepared silver NPs were tested as efficient catalysts for redox reactions. For this purpose, a model reaction, the reduction of organic dye by sodium borohydride was used. The mechanism of this reaction is discussed using the Langmuir–Hinshelwood model of heterogeneous catalysis.



■ INTRODUCTION

Silver nanoparticles (Ag NPs) are among nanomaterials that can be encountered in a daily life, most often as antimicrobial finishing of functional textiles.^{1,2} In addition to their antimicrobial activity, these nanoparticles exhibit interesting optical properties^{3,4} and high catalytic activities, especially in redox reactions.^{5,6} The aforementioned unique properties are strongly dependent on shapes and/or sizes of Ag NPs which can be fine-tuned to meet the demands of particular applications. In surface-enhanced Raman spectroscopy, the high enhancement effect is achieved with hundreds of nanometer-sized particles,⁷ or it is necessary to activate the nanoparticles by the addition of the substances that induce their aggregation or even recrystallization onto particles approximately 1 order of magnitude larger.^{8–10} On the other hand, the antimicrobial activity of Ag NPs increases with decreasing nanoparticle size.^{11,12} Catalytical action of nanoparticles represents particularly complex problematics. As reported in a variety of papers, the catalytical activity of silver nanoparticles increases with decreasing particle size, the maximum catalytical action being observed, e.g., for NPs with sizes as low as 5 nm in the case of anthracene catalytical hydrogenation¹³ or even below 1 nm in the case of the electrocatalytical reduction of

oxygen.¹⁴ Similar dependence of catalytical activity on particle size was observed also for Ag NPs anchored to inert carrier used to catalyze partial oxidation of propylene to propylene oxide and acrolein.¹⁵ Interestingly, in this case, it was shown that the size of the used Ag NPs influences not only the magnitude of the catalytical action, but also the selectivity toward the production of propylene oxide, which on the other hand rises with increasing particle size.

Because of the fact that individual applications utilizing Ag NPs have different demands on sizes and shapes of the used nanoparticles, reliable methods of their controllable syntheses are still researched. From this point of view the methods based on chemical reduction of silver salt in solution (i.e., “wet” preparation methods) predominate.^{16–19} The classical method of synthesis of Ag NPs with controlled particle sizes is based on a two-step reduction of silver salt, where silver particles formed by the primary reduction of the silver salt using a strong reducing agent are, in the second step, enlarged by further reduction using a weaker reduction agent.^{20,21} This way, it is

Received: February 24, 2013

Revised: December 20, 2013

Published: January 7, 2014

possible to prepare Ag NPs in the range of sizes from 20 to 170 nm, but the reproducibility of the procedure is, unfortunately, seemingly low.

One-step syntheses of Ag NPs are less demanding from the experimental point of view and provide more reproducible results. The methods based on the Tollens process, enabling researchers to prepare nanoparticles with controlled sizes in the range 20–50 nm²² or alternatively from 25 to 450 nm,^{9,12} represent reliable and uncomplicated procedures. However, the resulting dispersions of Ag NPs are frequently highly polydisperse, which can be a serious problem for certain applications. The production of Ag NPs with controlled size and low polydispersity is possible only in the presence of polymer or surfactant additives, modifying the growth of the forming nanoparticles during the reduction process.^{23–25} The synthesis of Ag NPs using polyol process at elevated temperature can be quoted as an example, where the size of silver particles can be controlled by the addition of poly(acrylic acid).²³ Using this method, it is possible to prepare silver nanoparticles with sizes from 4 to 20 nm based on the molecular weight and concentration of the used PAA together with the reducing power of the used polyol solvent. Using sodium dodecyl sulfate (SDS) as a modifier in the process of AgNO₃ reduction using NaBH₄ it was possible to control the sizes of the Ag NPs from 3 to 5 nm and achieve low polydispersities by the changes in the ratio between reaction components.¹³ The methods based on the reduction of insoluble silver species, namely Ag₂O, are also usable. Using the reduction of this compound by hydrogen at elevated temperature and pressure the AgNPs with sizes in a broad range from 15 to 120 nm were prepared by varying the reaction time.²⁶ A disadvantage is the fact that the method is demanding in terms of the usage of reactor and of the use of high temperature for the synthesis.

Recently, several scientific papers dealing with synthesis and growth mechanism of silver NPs have been published.^{23,27–31} Growth of silver clusters or small silver NPs formed during fast initial nucleation reaction phase into final stable particles by aggregation mechanism has been predominantly described in these reports for reaction systems including polymeric stabilizing agent,^{23,27–30} although papers dealing with unstabilized systems can be also found.^{27,31}

This work, on the contrary to preceding publications on the topic, introduces the simple and reliable one-step (single-step) preparation method of highly monodisperse Ag NPs in a broad range of sizes from 30 to 80 nm at the laboratory temperature. The size of the prepared Ag NPs is controlled by the concentration of the used polymer modifier, e.g., the poly(acrylic acid) with high molecular weight. The advantage of this original method is the low concentration of the used polymer modifier, 1×10^{-10} to 1×10^{-7} mol/L. The application potential of the nanoparticles is not limited by the presence of the modifier as evidenced by the preservation of high catalytic activity of the prepared nanoparticles (studied on the model reaction of methylene blue reduction by NaBH₄).

EXPERIMENTAL SECTION

Chemicals. For the synthesis of silver NPs, silver nitrate (99.9%, Sigma-Aldrich), ammonia (p.a., 27% [w/w] aqueous solution, Sigma-Aldrich), sodium hydroxide (p.a., Lachema, Czech Republic), poly(acrylic acid) (PAA) (M.W. 100 000; 35% (w/w) aqueous solution, Sigma Aldrich) and D-(+)-maltose monohydrate (p.a., Riedel-de Haen) were used without further purification. For the catalytic

reaction, methylene blue and NaBH₄ (both p.a., Sigma-Aldrich) were used. The solutions were prepared using deionized water (18 MΩ·cm, Millipore).

One-Step Synthesis of Silver NPs with Controlled Size.

Silver NPs were prepared according to previously published procedure using a Tollens reaction based synthesis consisting in the reduction of the complex cation [Ag(NH₃)₂]⁺ by D-maltose in alkaline medium.¹² The reaction mixture contained AgNO₃ (1×10^{-3} mol/L) and NH₃ (5×10^{-3} mol/L), its pH (11.5) was adjusted by the addition of NaOH solution into the reaction mixture (the concentration of NaOH was ca. 1×10^{-2} mol/L). The reaction was initiated by the addition of maltose (1×10^{-2} mol/L final concentration) and yielded silver NPs with the average size of 28 nm. Silver NPs with various sizes ranging from 36 to 77 nm were prepared by the modification of the aforementioned Tollens process consisting in the presence of long-chain poly(acrylic acid) in the reaction mixture. The PAA solution was added before the addition of the reducing substance at desired volume to achieve the final PAA concentrations in the range from 5×10^{-10} mol/L to 1.3×10^{-7} mol/L. All silver NP syntheses were performed at laboratory temperature (~25 °C), under vigorous stirring. The reaction times ranging from 5 to 15 min to achieve complete conversion depended on the used PAA concentration in the reaction mixture.

The average sizes and size distributions of the prepared silver NPs were determined by dynamic light scattering (DLS) using the Zetasizer Nano ZS (Malvern). The nanodimensions of the synthesized silver NPs were confirmed by transmission electron microscopy using the JEM-2010 (Jeol) and by UV-vis absorption spectroscopy with the Specord S 600 spectrophotometer (Analytik Jena AG). UV-vis spectroscopy was used to monitor kinetic curves of the reduction process yielding silver NPs and also for monitoring of catalytic reduction process of organic dyes by sodium borohydride. Kinetic curves of the reduction process yielding silver NPs were obtained for each PAA concentration by recording the increasing absorbance at the wavelength corresponding to absorption maximum for given size of silver NPs.

Electrochemical Measurements. Electrochemical measurements were performed on CH-Instruments model 660 C electrochemical workstation in a three electrode configuration. Ag/AgCl was used as a reference electrode (CHI111, CH Instruments), platinum wire served as an auxiliary and glassy carbon disk electrode (3 mm in diameter, CHI104, CH Instruments) as a working electrode. Working electrode was repolished using alumina slurry (0.05 μm) on Microcloth pad (both Buehler, U.S.A.) before each scan. Electrochemical measurements were conducted for solutions of AgNO₃, AgNO₃ with PAA, [Ag(NH₃)₂]⁺, and [Ag(NH₃)₂]⁺ with PAA. Concentrations of silver nitrate and ammonia were the same as in the reaction mixture used for the nanoparticle synthesis (1×10^{-3} mol/L and 5×10^{-3} mol/L, respectively) and the concentration of PAA was 1.3×10^{-7} mol/L.

Size-Dependent Catalytic Efficiency of Silver NPs. The catalytic activity of the prepared silver nanoparticles was studied using a model reaction based on the reduction of thiazine dye methylene blue (MB) by sodium borohydride. In the absence of silver nanoparticle catalyst, the reaction is very slow (halftime in the range of tens of minutes), catalysis by silver nanoparticles enhances the reaction rate even at temperatures below the laboratory temperature (halftimes in the range of tens of seconds). The catalytic activity of the prepared silver nanoparticles can thus be conveniently evaluated by continuous monitoring of the decrease in the absorbance of oxidized form of the dye which is reduced to its leuco form (see Figure S1 in the Supporting Information).

The individual kinetic experiments were carried out directly in 1 cm spectrophotometric cuvettes, placed in thermostatted cell holder of the spectrometer kept at 6 ± 0.2 °C. At this temperature the difference in the catalyzed vs uncatalyzed reaction was maximal. The high value of methylene blue absorption coefficient ($\epsilon = 95\,000$ at $\lambda = 664$ nm)³² enables to study the kinetics even at low (1×10^{-5} mol/L) initial MB concentration, at which the reaction half-times in units to tens of seconds are achieved, allowing for high precision of kinetic analyses in a given experimental setup. The reaction was initiated by injecting 1 mL of 0.01 mol/L NaBH₄ solution into 1 mL of MB solution in

ammoniacal buffer, pH 10; eventually containing AgNP catalyst the concentration of which was adjusted so that 3×10^{-8} mol/L Ag was present in the cuvette. All components of the reaction mixture were temperature equilibrated before the mixing and thermostatic control was provided also during the kinetic experiment. The spectrum of MB was recorded in regular interval in the wavelength range of 360–800 nm. Kinetic curves were constructed from the absorbance values at MB absorption maximum (664 nm).

RESULTS AND DISCUSSION

One-Step Synthesis of Silver NPs with Controlled Size.

Silver NPs with various sizes from 28 to 77 nm were prepared by improvement of modified Tollens process using poly(acrylic acid) (PAA) with a long polymer chain at different concentrations as an additive. The impact of PAA presence in the reaction mixture on the sizes of the prepared silver NPs was monitored by the determination of average size using DLS and by recording the absorption spectra. PAA showed itself to be a very effective tool to control the sizes of the prepared silver nanoparticles, even at very low concentrations, as documented in Figure 1 and Table S1 in the Supporting Information. In the

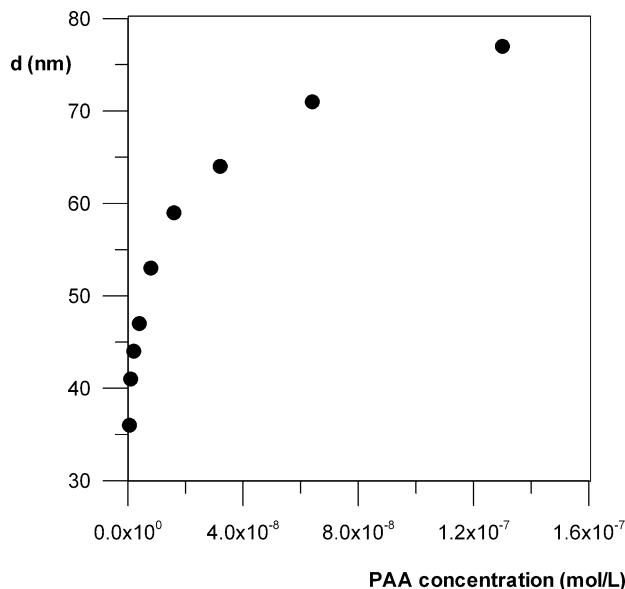


Figure 1. Size dependence of silver NPs on the concentration of poly(acrylic acid) in the reaction system.

absence of PAA, the reaction provided silver NPs with 28 nm average size. In the presence of PAA, even at the lowest used concentration (5×10^{-10} mol/L), the average size increased by ca. 30%, i.e., from 28 to 36 nm. With further increasing concentration of PAA in the reaction mixture the average size of the prepared silver colloid particles grew gradually from 36 nm up to 77 nm for the highest used PAA concentration (1.3×10^{-7} mol/L).

The sizes of the prepared NPs were confirmed by electron microscopy – TEM images of colloid particles prepared in the absence of PAA (average size 28 nm), in the presence of PAA at the concentration of 5×10^{-10} mol/L (36 nm), 8×10^{-9} mol/L (53 nm), and 1.3×10^{-7} mol/L (77 nm) are shown in Figure 2. The observed dependence of particle size on the PAA concentration in the reaction mixture has a typical logarithmic course, where at higher PAA concentrations (above 1×10^{-8} mol/L) only slight changes in the average sizes are observed. At the highest studied PAA concentration of 1.3×10^{-7} mol/L,

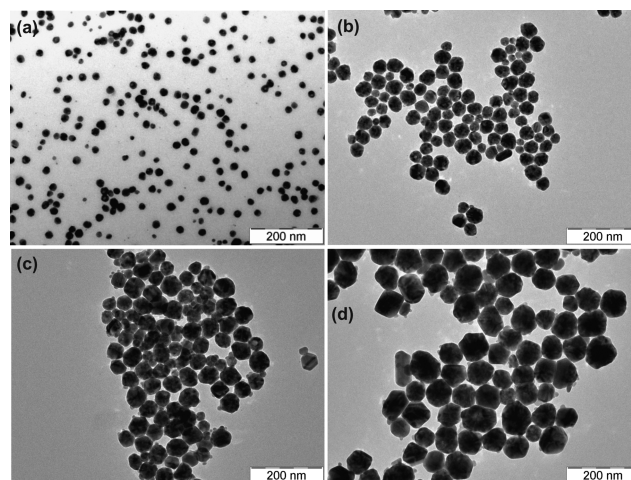


Figure 2. TEM images of silver NPs prepared (a) without poly(acrylic acid) and with a poly(acrylic acid) at following concentrations (b) 5×10^{-10} , (c) 8×10^{-9} , and (d) 1.3×10^{-7} mol/L.

the Ag NP size reaches the mean value of 77 nm, i.e., ca. three times higher value than without PAA.

The changes in sizes of the prepared silver nanoparticles in dependence on PAA concentration in the reaction system are reflected also in their optical properties. In the absorption spectra, a decrease in absorbance and also a shift in maxima of surface plasmon toward higher wavelengths occurred when the mean value of silver nanoparticle sizes was increased (see Figure S2 in the Supporting Information). The surface plasmon of spherical silver nanoparticles with 28 nm mean size (without PAA) is localized at 407 nm and shifts with growing nanoparticle size toward 450 nm for 77 nm sized nanoparticles. Shift of the surface plasmon of silver NPs with increasing size is in accordance with experimental absorption spectra of differently sized silver nanoparticles available in the literature.²¹

With increasing concentration of PAA in the reaction system a slowdown in the reaction rate is observed (Figure 3) from

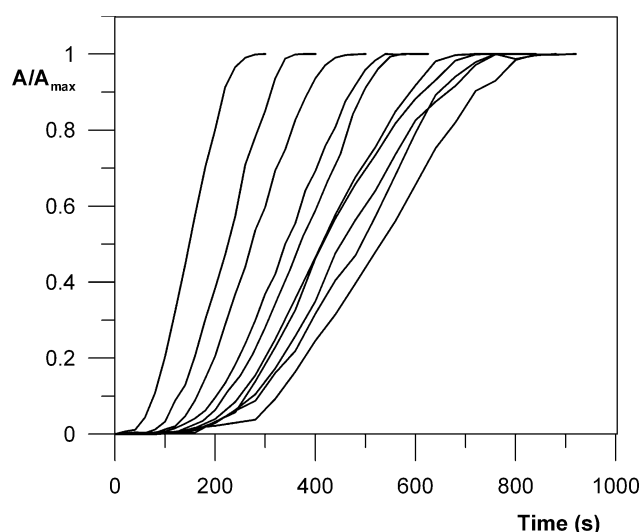


Figure 3. Kinetic curves monitoring the $[\text{Ag}(\text{NH}_3)_2]^+$ reduction process by maltose at different concentrations of poly(acrylic acid). The first curve from the left belongs to the reaction without PAA and the other ones belong to reactions carried out with increasing concentrations of poly(acrylic acid).

230 s pertaining to the reaction system without PAA (yielding 28 nm sized silver NPs) up to 900 s for the reaction mixture containing PAA at the highest used concentration (yielding 77 nm sized silver NPs). The decrease in the overall reaction rate is connected with decrease in the reaction rate of the fast reaction stage (growth of the nuclei to final nanoparticles) and also with prolongation of the initiation phase of the reduction process (phase of the formation of the stable nuclei). It can therefore be assumed that presence of PAA influenced both initiation phase of new nuclei formation and their subsequent growth in the following fast reaction stage.

Slowdown in the overall reaction rate has two reasons. At the first prolongation of the initiation phase of the reduction process (phase of the formation of the stable nuclei) is caused by the strong binding of silver ion into a stable complex compound formed by NH₃ and PAA. The concentration of free silver ions available for the reduction is influenced not only by ammonia but also by the PAA present in the reaction mixture. Apparently, PAA behaves as complexing agent forming the complex with stronger bonds than the diammunesilver(I) complex. This fact was proved using the electrochemical technique of cyclic voltammetry. Voltammetric measurements are an elegant way of characterizing the redox behavior of coordination compounds. Provided that simple reduction of a metal ion to the metal occurs, increasing stability of the complex shifts the electrochemical reduction of the central metal ion toward a more negative potential. Alternatively, if the redox transformation proceeds without breaking ligand-central metal ion bonds, the formal potentials mirror the ratio of the complex stability constants of the two oxidation states.³³ Cyclic voltammograms of silver nitrate in the presence of NH₃, PAA and both PAA and NH₃ are shown in Figure 4.

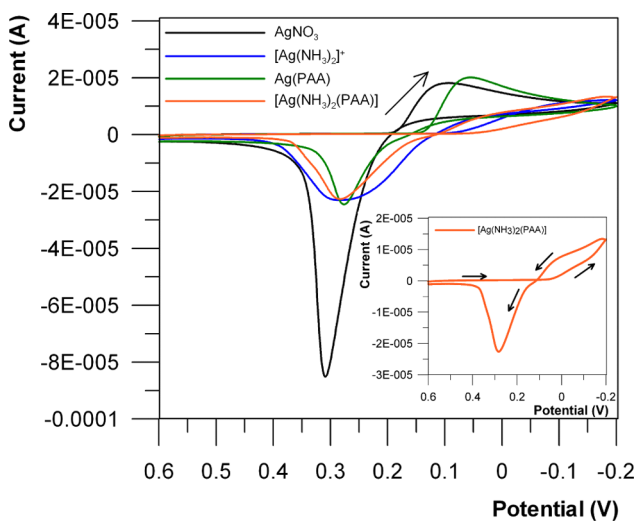


Figure 4. Cyclic voltammograms of AgNO₃ (10^{-3} mol/L) and also AgNO₃ in the presence of NH₃ (5×10^{-3} mol/L), PAA (1.3×10^{-7} mol/L), and both PAA and NH₃ (arrow drawn near the cathodic peak indicates the direction of the forward scan).

The voltammograms reveal the cathodic peaks corresponding to the reduction of silver ion to silver metal deposited on the electrode and (sharper) anodic peaks corresponding to stripping of the metallic silver accumulated on the electrode surface which are observed in the reverse scans. Apparently, binding the Ag⁺ ion into complexes with PAA (1.3×10^{-7} mol/L) and NH₃ (5×10^{-3} mol/L) causes shifts of the cathodic

peaks toward negative potentials compared to the position of the peak of free Ag⁺ which is the evidence of strong complexing of Ag⁺ ion by these complexing agents. The onsets of the cathodic peaks alongwith the values of cathodic peak potentials (E_{pc}) are shown in Table 1.

Table 1. Onsets of Cathodic Peaks (mV) and Cathodic Peak Potentials (mV) of AgNO₃ Alone and AgNO₃ in the Presence of PAA (1.3×10^{-7} mol/L), NH₃ (5×10^{-3} mol/L), and both PAA and NH₃

	onset of cathodic peak (mV)	E_{pc} (mV)
AgNO ₃	190	90
+ PAA	150	50
+ NH ₃	80	-200
+ PAA and NH ₃	50	<-200

Additionally, only in the case of the voltammogram recorded in the mixture of NH₃ and PAA, the cathodic current of complexed Ag⁺ ions in the reverse scan is greater than the cathodic current in the first part of voltammetric cycle (pronounced “trace crossing”, see inset in Figure 4), implicating that the rate determining step for reduction of Ag⁺ ions on electrode is nucleation or addition of the new silver atoms onto electrode surface.³⁴ From the cyclic voltammetry measurements, it can thus be concluded that the mixture of NH₃ with PAA significantly influences (retards) the nuclei formation and their subsequent growth in the course of the silver reduction process.

Cyclic voltammetry therefore shows that PAA not only does influence the initial phase of stable nuclei formation (formation of stable complex with Ag⁺) but also suggests the second cause of the slowdown in the overall reaction rate, i.e., the inhibition of the fast reaction stage of the nuclei growth to final nanoparticles. At this stage, PAA retards addition of new silver atoms onto growing silver nuclei. Assuming rapid adsorption of PAA onto the surface of growing nuclei, the adsorption layer formation would result in the retardation of the growth of these nuclei by the heterogeneous mechanism in which these nuclei serve as catalytic sites for the reduction of Ag⁺ ions. If heterogeneous catalytic reduction of the Ag⁺ on the surface of the growing nuclei is retarded by the adsorption layer of PAA the formation of new nuclei via homogeneous mechanism should occur, as suggested in Figure 5. The silver cations are drawn close to the surface of primarily formed silver particles due to electrostatic interaction with negatively charged carboxyl groups and they are subsequently reduced by the maltose forming new silver nuclei. These new nuclei are very closely packed around of the primary silver particles which is the main reason for the starting the aggregation mechanism of additional growth of these primarily formed silver particles. The used low concentrations of PAA polymer (the highest used concentration is 0.0013% [w/w]) are not sufficient to prevent this aggregation process as several orders higher concentrations are needed to stabilize the nanoparticles effectively against aggregation.³⁵ The applicability of this hypothesis of the mechanism of silver particle secondary growth is supported by TEM images showing the silver nanoparticles in different growth stages (Figure 6). The samples were taken out from the reaction mixture with PAA concentration of 1.3×10^{-7} mol/L after 2 min (Figure 6A), and 5 min. (Figure 6B) (followed by 2 min of drying under vacuum) from the initiation of the reaction. The sample shown in Figure 6C was collected after

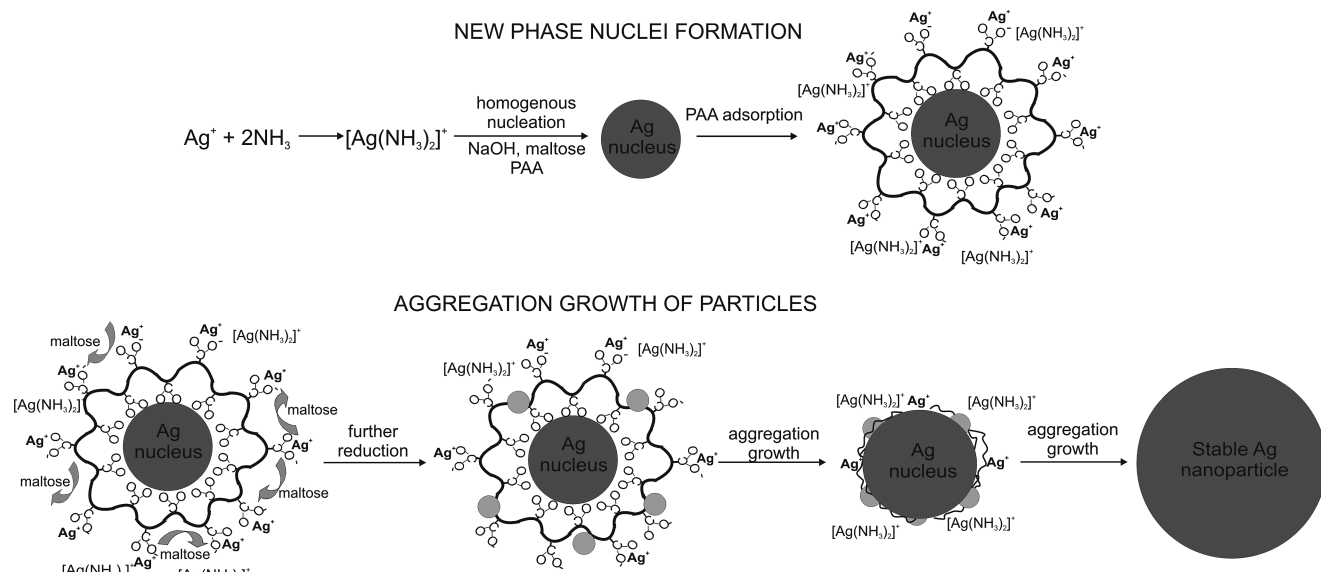


Figure 5. Scheme of the mechanism of the silver nanoparticle growth in the presence of PAA.

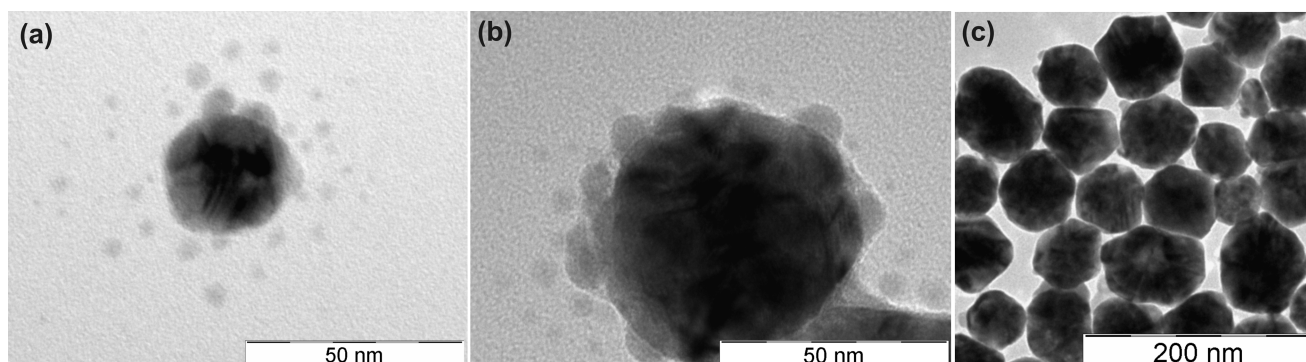


Figure 6. TEM images capturing (a, b) aggregation growth of silver nanoparticle into (c) stable silver nanoparticles with an average size of 77 nm.

the completion of the reaction, i.e., after 15 min. Newly formed nuclei of ca. 3–8 nm are discernible in Figure 6A in the vicinity of primary silver particle, which subsequently grows due to aggregation with these secondary particles (Figure 6B) to result in the stable nanoparticles of 77 nm size (Figure 6C).

Apart from electron microscopy the suggested mechanism is supported also by the observation of changes in the optical properties of the forming nanoparticles. Figure S3 in the Supporting Information shows the absorption spectra recorded during the whole reduction process carried out in the presence of PAA (1.3×10^{-7} mol/L). In the first four minutes of the reaction the absorption maximum belonging to surface plasmon is localized at 415 nm. This maximum is shifted toward longer wavelengths with growing NP size up to 450 nm which is a value typical for the final 77 nm particles.²¹ From these observations one can deduce that in the initial stages of the reduction process small particles are present in the reaction mixture, growing into bigger particles in subsequent stage of the rapid particle growth. The particle growth mechanism based on the aggregation process could cause these changes in UV-vis spectra which is in good accordance with previously published reports.^{27–31}

In summary, the explanation of the PAA effect on final size of the silver NPs is based on several different action modes of the polymer on the reaction course of Ag^+ reduction. The first

complexation of Ag^+ ions by a mixture of NH_3 and PAA causes the prolongation of the initiation phase of the reduction process (phase of the formation of the stable nuclei). And increasing the concentration of PAA in the reaction system causes slowdown of process of primary nanoparticles formation in initial stage of reaction. More PAA in the system results in formation of less nuclei (or primary nanoparticles) and therefore bigger final nanoparticles are formed because of the fact that the same amount of silver is divided into fewer nanoparticles.

The second PAA adsorption on the surface of the primarily formed silver nuclei retards their subsequent growth by the mechanism of adding additional Ag atoms reduced on the surface of silver particle. Therefore, the secondary silver nuclei are formed in the vicinity of surface of primarily formed silver nanoparticles, which subsequently aggregate together to form bigger silver nanoparticles. In this secondary process, the electrostatic interactions Ag^+ ions with negatively charged PAA molecule play an irreplaceable role, which was confirmed by additional experiments, in which PAA was replaced by nonelectrolyte polymer, specifically the polyethylene glycol of molecular weight 35 kDa. No effect on resulting sizes of silver NPs was observed in this case. The size of produced silver NPs was not influenced by the polymer concentration and it was

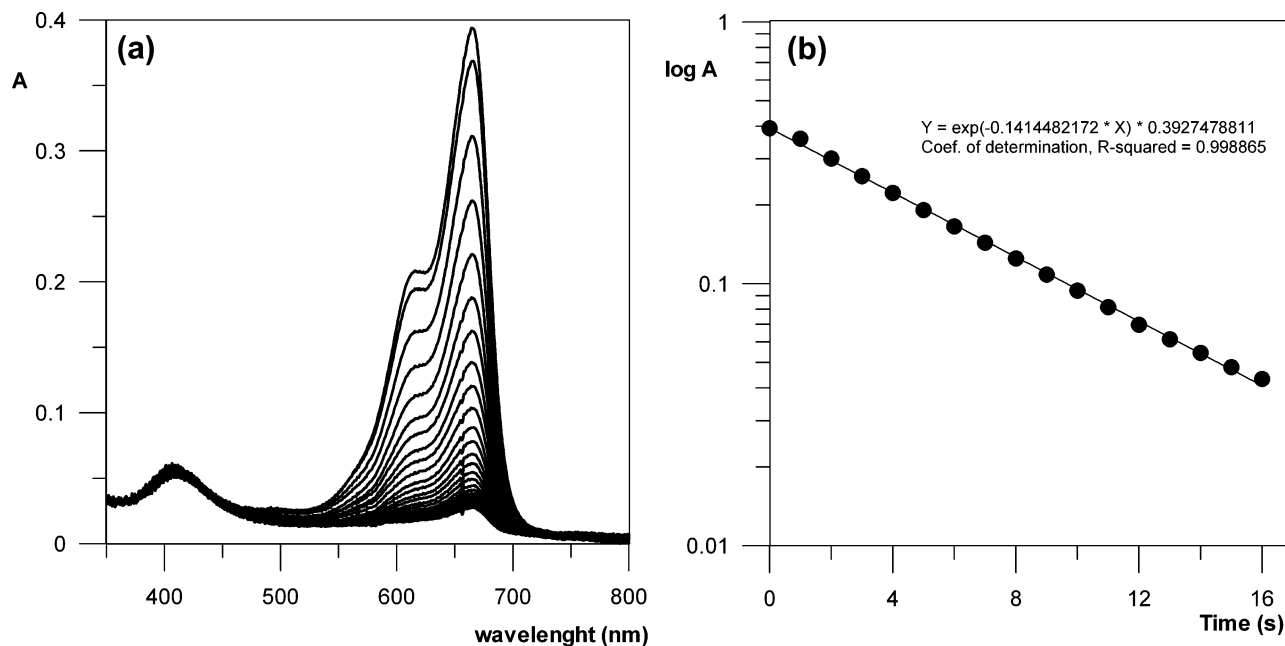


Figure 7. (a) Time course of the change in the absorption spectra of methylene blue solution ($c_0 = 1 \times 10^{-5}$ mol/L) during the reduction of methylene blue by NaBH_4 in the presence of silver nanoparticles (36 nm mean size) as catalyst and (b) corresponding kinetic curve obtained from absorbance values determined in the absorption maximum at 664 nm.

constant, approximately 30 nm in the range of PEG concentrations of 1×10^{-10} to 1×10^{-5} mol/L.

Size-Dependent Catalytic Efficiency of Silver NPs

Catalytic activity of silver nanoparticles is mostly studied using model reactions, which enable effective execution of kinetic studies. Among reactions often used from this point of view is the reduction of 4-nitrophenol to 4-aminophenol^{6,36} or the reduction of thiazine dyes, e.g. methylene blue.^{37,38} In this study, the reduction of thiazine dye methylene blue (see Figure S1 in the Supporting Information) by NaBH_4 is used as suitable model reaction because the absorption maxima of the used dye do not coincide with absorption maximum of surface plasmon of silver nanoparticles. This fact greatly simplifies both spectrophotometric assay of the reaction kinetics and also the kinetic data evaluation. To achieve a high degree of kinetic experiment reproducibility, we carried out the model reactions at lowered temperature ($6 \pm 0.2^\circ\text{C}$). At this temperature, the reaction rate is optimal for the simple spectrophotometric monitoring without special experimental equipment for study of fast chemical reactions and at the same time the hydrolysis of the reducing agent is suppressed, significantly improving the reproducibility of the kinetic experiments. The reaction was initiated by the addition of the solution of reducing agent into the cuvette containing all components of the reaction mixture including tested catalyst (silver NPs) and the course of the reaction was followed through decreases in the absorption maxima of the dye the reduced form of which is colorless. A typical recording of the kinetic experiment is shown in Figure 7a for methylene blue reduced by NaBH_4 under the catalysis of silver nanoparticles of 36 nm mean size. Because the reduced form of methylene blue is colorless and the absorbance of oxidized form (664 nm absorption maximum) obeys the Lambert–Beer's law, it is possible to construct the kinetic curves of the studied reaction as dependencies of absorbance on the reaction time (Figure 7b). Typical kinetic curves for all sizes of prepared silver NPs are presented in the Supporting Information (Figures S4–S6).

The mechanism of the studied catalytical reaction involves the adsorption of reactants onto the surface of metal nanoparticle, which mediates the electron transfer between reductant molecule (NaBH_4) and reduced dye molecule (MB). In the case of BH_4^- anion, the adsorption is a reversible and fast process; therefore, it can be well-described by the Langmuir adsorption isotherm.³⁹ The same law governs the adsorption of the dye molecule onto nanoparticle surface. The whole process can thus be described using Langmuir–Hinshelwood model of heterogeneous catalytic process, where both reactants are adsorbed on the surface of catalyst⁴⁰

$$\nu = -\frac{dC_A}{dt} = -\frac{dC_B}{dt} = \frac{kK_A K_B C_A C_B}{(1 + K_A C_A + K_B C_B)^2} S^2 \quad (1)$$

where k is the rate constant of the studied reaction, S is the surface of the catalyst, K_A and K_B adsorption coefficients, and C_A and C_B are the concentrations of reactants in the reaction mixture. The concentration of the dye is very low with respect to borohydride concentration (ca. 100 excess of borohydride); therefore, the kinetic eq 1 can be simplified on the basis of the assumption of weak dye adsorption in comparison to BH_4^- adsorption, i.e., $K_A C_A \ll K_B C_B$:

$$\nu = \frac{k K_A K_B C_A C_B}{(1 + K_B C_B)^2} S^2 \quad (2)$$

From eq 2, it follows that the partial reaction order will be one with respect to the dye concentration C_A . When including all constants as well as C_B into an overall constant k' , eq 2 simplifies into a well-known first-order kinetic equation

$$\nu = k' C_A \text{ or } \frac{C_A}{C_{A,0}} e^{-k't} \quad (3)$$

where newly introduced rate constant k' is

$$k' = \frac{k K_A K_B C_B}{(1 + K_B C_B)^2} S^2 \quad (4)$$

This simplification enables facile evaluation of the experimental kinetic curves using regression of the exponential function, corresponding to integrated first-order kinetic equation. The apparent rate constants k' obtained this way should be proportional to the square of the surface area of the catalyst (eq 4) as is predicted from the Langmuir–Hinshelwood kinetic model (eq 1). Consequently, the dependence of the apparent rate constants k' on the total surface area of the used catalyst (i.e., AgNPs) present in the reaction mixture was evaluated by nonlinear regression using a model of power law $y = ax^b$ (which is a simplified eq 4), where y stands for k' and x for total surface area of catalyst S . This regression yields the exponent value b of 1.99 (Figure 8), confirming the assumption of the Langmuir–

of the catalyzing silver NPs, i.e. $S = f(d^{-1})$. From this and the above-mentioned dependency of catalytic activity on the total surface area, one can conclude that the reaction rate should decrease with square of particle size, i.e., $k' = f(d^{-2})$. The value of -1.99 was obtained from nonlinear regression of the experimental data (see Figure S7 in the Supporting Information) using a model of power law $y = ax^b$, where y stands for k' and x for diameter d of silver NPs. Again, very good correspondence of this experimentally obtained value with theory confirms the assumption of usability Langmuir–Hinshelwood model for the studied catalytic reaction.

■ CONCLUSION

The possibility of the simple and rapid synthesis of silver NPs in wide range of sizes from 28 to 77 nm was described. The resulting size of the prepared particles was simply controlled by the concentration of long-chain poly(acrylic acid) which was used as growth modifier in this new synthetic method. It was found that poly(acrylic acid) influences not only the process of new nuclei formation in the initial stage of the reaction but also subsequent growth of the particles up to the final size of the formed nanoparticle. The homogeneous process of nucleation is influenced by the formation of strongly bound complex between silver ions and PAA in the presence of excess ammonia, which was proven by cyclic voltammetry measurements. The aggregation mechanism of particle growth in further stage of reaction was suggested based on the conception of adsorption layer of polymer which blocks direct interaction of silver ions with surface of primarily formed nuclei. This way, the heterogeneous reduction of silver ions is hindered and cannot act as a process of subsequent nuclei growth. Therefore, new nuclei are formed by homogeneous mechanism in the vicinity of the polymer adsorption layer which then aggregate with the primarily formed silver nuclei to form the resulting silver nanoparticles. Subsequently conducted study of size-dependent catalytic efficiency of the prepared silver NPs revealed that in the studied range of nanoparticle sizes between 28–76 nm the catalytical activity is unambiguously dependent on the total surface area of the nanoparticles present in the system. The process is governed by Langmuir–Hinshelwood mechanism of the heterogeneous catalysis.

■ ASSOCIATED CONTENT

Supporting Information

Table S1 and Figures S1–S7. This material is available free of charge via the Internet at <http://pubs.acs.org>.

■ AUTHOR INFORMATION

Corresponding Author

*E-mail: libor.kvitek@upol.cz.

Author Contributions

All authors have given approval to the final version of the manuscript.

Notes

The authors declare no competing financial interest.

■ ACKNOWLEDGMENTS

The authors gratefully acknowledge the support by the Operational Program Research and Development for Innovations - European Regional Development Fund (project CZ.1.05/2.1.00/03.0058 of the Ministry of Education, Youth and Sports of the Czech Republic), by the Operational Program

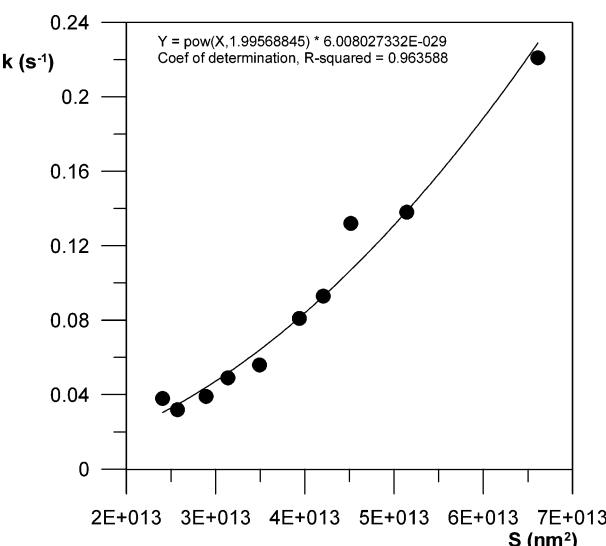


Figure 8. Dependence of apparent rate constant k' of the methylene blue reduction by NaBH_4 on the total surface area of silver nanoparticles added into the reaction mixture as a catalyst.

Hinshelwood mechanism of heterogeneous catalysis (eqs 2 and 4) where the rate of the reaction is proportional to the power two of the total surface area of heterogeneous catalyst. The total surface area of the AgNPs catalyst in the reaction mixture was calculated assuming uniform size and ideal spherical shape of the nanoparticles, the dimensions of which are equal to an average size determined by DLS (see Table S1 in the Supporting Information).

The obtained results of kinetic experiments prove unequivocally, that the catalytic action of tens of nanometers sized silver nanoparticles is dependent on their surface area, and is not influenced by the changes in other physicochemical parameters, e.g., the dependence of redox potential on particle size, as it was observed for units of nanometers sized nanoparticles.⁴¹ This conclusion can be further supported by the dependence of apparent rate constant k' of the studied reaction on the size of silver nanoparticles used as catalyst (see Figure S7 in the Supporting Information). The reason for the decrease of reaction rate with growing size of the silver NPs is a cubic decrease in the total number of silver NPs N with their growing size due to the fact that the total amount of silver in the reaction system is constant. Therefore, total surface area of the silver NPs is indirectly proportional to the size (diameter d)

Education for Competitiveness - European Social Fund (project CZ.1.07/2.3.00/20.0056 of the Ministry of Education, Youth and Sports of the Czech Republic), by Czech Science Foundation (GAP304/10/1316) and by Internal Grant of Palacky University in Olomouc (PrF_2013_031).

■ REFERENCES

- (1) Dastjerdi, R.; Montazer, M. *Colloids Surf, B* **2010**, *79*, 5.
- (2) Chen, X.; Schluesener, H. J. *Toxicol. Lett.* **2008**, *176*, 1.
- (3) Kelly, K. L.; Coronado, E.; Zhao, L. L.; Schatz, G. C. *J. Phys. Chem. B* **2003**, *107*, 668.
- (4) Lee, K. S.; El-Sayed, M. A. *J. Phys. Chem. B* **2006**, *110*, 19220.
- (5) Chimentao, R. J.; Kirm, I.; Medina, F.; Rodriguez, X.; Cesteros, Y.; Salagre, P.; Sueiras, J. E. *Chem. Comun.* **2004**, *7*, 846.
- (6) Pradhan, N.; Pal, A.; Pal, T. *Colloids Surf, A* **2002**, *196*, 247.
- (7) Michaels, A. M.; Nirmal, M.; Brus, L. E. *J. Am. Chem. Soc.* **1999**, *121*, 9932.
- (8) Cunningham, D.; Littleford, R. E.; Smith, W. E.; Lundahl, P. J.; Khan, I.; McComb, D. W.; Graham, D.; Laforest, N. *Faraday Discuss.* **2006**, *132*, 135.
- (9) Kvitek, L.; Prucek, R.; Panacek, A.; Novotny, R.; Hrbac, J.; Zboril, R. *J. Mater. Chem.* **2005**, *15*, 1099.
- (10) Prucek, R.; Panacek, A.; Fargasova, A.; Ranc, V.; Masek, V.; Kvitek, L.; Zboril, R. *CrystEngComm* **2011**, *13*, 2242.
- (11) Morones, J. R.; Elechiguerra, J. L.; Camacho, A.; Holt, K.; Kouri, J. B.; Ramirez, J. T.; Yacaman, M. J. *Nanotechnology* **2005**, *16*, 2346.
- (12) Panacek, A.; Kvitek, L.; Prucek, R.; Kolar, M.; Vecerova, R.; Pizurova, N.; Sharma, V. K.; Nevecna, T.; Zboril, R. *J. Phys. Chem. B* **2006**, *110*, 16248.
- (13) Deng, J. P.; Shih, W. C.; Mou, C. Y. *J. Phys. Chem. C* **2007**, *111*, 9723.
- (14) Lu, Y. Z.; Chen, W. *J. Power Sources* **2012**, *197*, 107.
- (15) Molina, L. M.; Lee, S.; Sell, K.; Barcaro, G.; Fortunelli, A.; Lee, B.; Seifert, S.; Winans, R. E.; Elam, J. W.; Pellin, M. J.; Barke, I.; von Oeynhausen, V.; Lei, Y.; Meyer, R. J.; Alonso, J. A.; Rodriguez, A. F.; Kleibert, A.; Giorgio, S.; Henry, C. R.; Meiwas-Broer, K. H.; Vajda, S. *Catal. Today* **2011**, *160*, 116.
- (16) Evanoff, D. D.; Chumanov, G. *ChemPhysChem* **2005**, *6*, 1221.
- (17) Guo, S. J.; Wang, E. K. *Nano Today* **2011**, *6*, 240.
- (18) Tao, A. R.; Habas, S.; Yang, P. D. *Small* **2008**, *4*, 310.
- (19) Wilcoxon, J. P.; Abrams, B. L. *Chem. Soc. Rev.* **2006**, *35*, 1162.
- (20) Shirtcliffe, N.; Nickel, U.; Schneider, S. *J. Colloid Interface Sci.* **1999**, *211*, 122.
- (21) Schneider, S.; Halbig, P.; Grau, H.; Nickel, U. *Photochem. Photobiol.* **1994**, *60*, 605.
- (22) Yin, Y. D.; Li, Z. Y.; Zhong, Z. Y.; Gates, B.; Xia, Y. N.; Venkateswaran, S. *J. Mater. Chem.* **2002**, *12*, 522.
- (23) Hu, Y. X.; Ge, J. P.; Lim, D.; Zhang, T. R.; Yin, Y. D. *J. Solid State Chem.* **2008**, *181*, 1524.
- (24) Huber, K.; Witte, T.; Hollmann, J.; Keuker-Baumann, S. *J. Am. Chem. Soc.* **2007**, *129*, 1089.
- (25) Kiryukhin, M. V.; Sergeev, B. M.; Prusov, A. N.; Sergeyev, V. G. *Polym. Sci., Ser. B* **2000**, *42*, 158.
- (26) Evanoff, D. D.; Chumanov, G. *J. Phys. Chem. B* **2004**, *108*, 13948.
- (27) Polte, J.; Tuaev, X.; Wuithschick, M.; Fischer, A.; Thuenemann, A. F.; Rademann, K.; Krahnert, R.; Emmerling, F. *ACS Nano* **2012**, *6*, 5791.
- (28) nLiu, T.; Li, D. S.; Yang, D. R.; Jiang, M. H. *Mater. Lett.* **2011**, *65*, 628.
- (29) Kochkar, H.; Aouine, M.; Ghorbel, A.; Berhault, G. *J. Phys. Chem. C* **2011**, *115*, 11364.
- (30) Richards, V. N.; Rath, N. P.; Buhro, W. E. *Chem. Mater.* **2010**, *22*, 3556.
- (31) Schenck, J.; Trobs, L.; Emmerling, F.; Kneipp, J.; Panne, U.; Albrecht, M. *Anal. Methods* **2012**, *4*, 1252.
- (32) Cenens, J.; Schoonheydt, R. A. *Clays Clay Miner.* **1988**, *36*, 214.
- (33) Pombeiro, A. J. L.; McCleverty, A. J. *Molecular Electrochemistry of Inorganic, Bioinorganic and Organometallic Compounds*; NATO ASI Series C; Kluwer, Dordrecht, The Netherlands, 1993; Vol. 385.
- (34) Noel, M.; Vasu, K. I. *Cyclic Voltammetry and The Frontiers of Electrochemistry*; Oxford and IBH Publishing: New Delhi, India, 1990.
- (35) Kvitek, L.; Panacek, A.; Soukupova, J.; Kolar, M.; Vecerova, R.; Prucek, R.; Holecova, M.; Zboril, R. *J. Phys. Chem. C* **2008**, *112*, 5825.
- (36) Zhang, W.; Tan, F. T.; Wang, W.; Qiu, X. L.; Qiao, X. L.; Chen, J. G. *J. Hazard. Mater.* **2012**, *217*, 36.
- (37) Ghosh, S. K.; Kundu, S.; Mandal, M.; Pal, T. *Langmuir* **2002**, *18*, 8756.
- (38) Yuan, G. Q.; Chang, X. Y.; Zhu, G. J. *Particuology* **2011**, *9*, 644.
- (39) Zhang, J. S.; Delgass, W. N.; Fisher, T. S.; Gore, J. P. *J. Power Sources* **2007**, *164*, 772.
- (40) Atkins, P.; Paula, J. d. *Atkins' Physical Chemistry*, 8th ed.; Oxford University Press: New York, 2006; p 998.
- (41) Sau, T. K.; Pal, A.; Pal, T. *J. Phys. Chem. B* **2001**, *105*, 9266.